International Geology Review, Vol. 46, 2004, p. 795–816.

Serpentinites, Peridotites, and Seismology

NIKOLAS I. CHRISTENSEN[1]

Department of Geology and Geophysics, University of Wisconsin, Madison, Wisconsin 53706

Abstract

Understanding the physical properties of ultramafic rocks is important for evaluating the wide variety of petrologic models for the Earth's upper mantle and lower oceanic crust. At comparable temperatures and pressures, velocities of compressional and shear waves in ultramafic rocks decrease with increasing serpentinization. A major factor affecting these velocities is the variety of serpentine present. Antigorite, the serpentine species stable at high temperatures, has higher velocities and a lower Poisson's ratio than the serpentine polymorphs lizardite and chrysotile. In addition, seismic properties of ultramafic rocks vary with their proportion of olivine to pyroxene and abundances of accessory minerals formed during serpentinization, such as brucite, magnetite, magnesite, tremolite, and talc. Seismic anisotropy is an important property of relatively unaltered peridotites. Large, well-exposed ultramafic massifs provide the best information on the nature of upper mantle compressional wave anisotropy and shear wave splitting. Average compressional wave anisotropy in these massifs is approximately 5%. Shear wave splitting magnitudes vary significantly with propagation direction. The major lithologies present in much of the lower ocean crust are metadiabase and gabbro. Lizardite-chrysotile–bearing serpentinites are abundant, however, in regions that have allowed penetration of sea water into the upper mantle. Dehydration of subducting slabs and the rising of released fluids have resulted in hydrothermal alteration and a lowering of velocities in forearc mantle wedges. In addition to serpentinization, high pore pressures and metamorphism producing chlorite are required to explain the seismic properties of the forearc upper mantle.

Introduction

> Geochemists, geologists, and geophysicists have all drawn up hypotheses for the constitution and history of the interior of the Earth, adjusted to fit the facts with which they are familiar and to take account of those interpretations and principles which seem most cogent to them. The result is a variety of earth models, seemingly sufficiently diverse and attractive to fit every taste. (Buddington, 1943)

THIS QUOTATION, from a presidential address to the Mineralogical Society of America, applies equally well today to the vast literature dealing with the role of serpentinites and peridotites in the Earth's crust and upper mantle.

In the six decades following Buddington's presidential address, rock and mineral physical properties have played a key role in evaluating Earth models. The purpose of this paper is to examine the seismic properties of rocks ranging from peridotite to serpentinite. Emphasis is placed on relating mineralogy and preferred mineral orientations to ultramafic rock compressional (Vp) and shear (Vs) wave velocities and their anisotropies, and using these relations to interpret seismic velocities. The first question to be discussed is the effect of serpentinization on velocities and Poisson's ratio. New velocity data are presented for some common accessory minerals formed during serpentinization. Velocities and Poisson's ratios are compared for the rock-forming serpentines lizardite, chrysotile, and antigorite. Next, the effects of anisotropy on models relating velocity to percentage serpentinization are evaluated using anisotropies determined from multiple field-oriented samples from two large, well-exposed ultramafic massifs, Red Hills, New Zealand and Twin Sisters, USA. Finally, the problem of inferring serpentine abundance directly from velocities is considered briefly for the oceanic crust and the upper mantle along convergent margins.

Seismic Properties of Ultramafic Rocks

Our most detailed information on the deep crust and uppermost mantle comes from the interpretation of seismic data. In interpreting structure and seismic

[1]Email: chris@geology.wisc.edu

0020-6814/04/757/795-22 $25.00

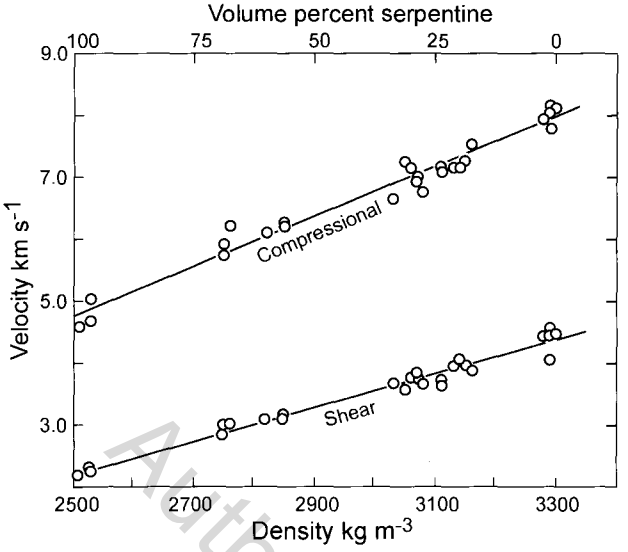

FIG. 1. Velocities at 1 GPa versus volume percent serpentine and density for peridotites and lizardite-chrysotile serpentinites (modified from Christensen, 1966).

velocities of a region, seismologists must focus on rock composition, a property of fundamental importance in understanding tectonic history. A careful juxtaposition of laboratory-measured velocities of common rock types with field-measured velocities enables us to decide which lithologies do not fit and, guided by petrologic considerations, which lithologies are at least not inconsistent with the seismic model. To be successful, this approach requires knowledge of velocities of rocks and minerals at appropriate temperatures and pressures as well as phase diagrams for pertinent mineral systems.

Serpentinization and Seismic Velocities

Early investigations found that serpentinites have significantly lower compressional wave velocities than unaltered peridotites and dunites. Hess (1959) estimated the compressional wave velocity of serpentine to be 5.8 km/s, whereas Birch (1961) found that relatively pure serpentine aggregates have velocities of approximately 6.0 km/s at 1 GPa. Christensen (1966) measured densities and both compressional (Vp) and shear (Vs) wave velocities for a suite of ultramafic rocks ranging from relatively pure lizardite-chrysotile serpentinites to unaltered peridotite. Velocities were measured at confining pressures of atmospheric to 1 GPa and in multiple directions to account for possible anisotropy. The results of this study are shown in Figure 1 for velocities at 1 GPa. Note that Vp systematically decreases with increasing serpentinization from approximately 8.3 km/s to 5.0 km/s. This wide range in Vp covers practically all velocities observed in the crystalline portions of the crust as well as the uppermost mantle. Thus, using only compressional wave velocities, it is possible for the seismologist to equate any crustal or upper mantle velocity between 5.0 and 8.3 km/s to ultramafic rocks that have undergone an appropriate degree of serpentinization. Shear wave velocities also decrease significantly with increasing serpentinization (Fig. 1) and the ratio Vp/Vs systematically increases from 1.78 to 2.21 with increasing serpentinization.

The elastic properties of isotropic solids are defined in terms of several elastic moduli, one being Poisson's ratio (σ), which can be calculated from Vp/Vs using the expression:

$$\sigma = 0.5[1 - 1/(\phi^2 - 1)], \text{ where } \phi = \text{Vp/Vs}.$$

This gives the following values of Vp/Vs for a range of possible Poisson's ratios

σ	0.0	0.1	0.2	0.3	0.4	0.5
Vp/Vs	1.414	1.500	1.633	1.871	2.449	∞

A value of $\sigma = 0.25$ has often been used in studies of the elastic properties of the Earth's mantle.

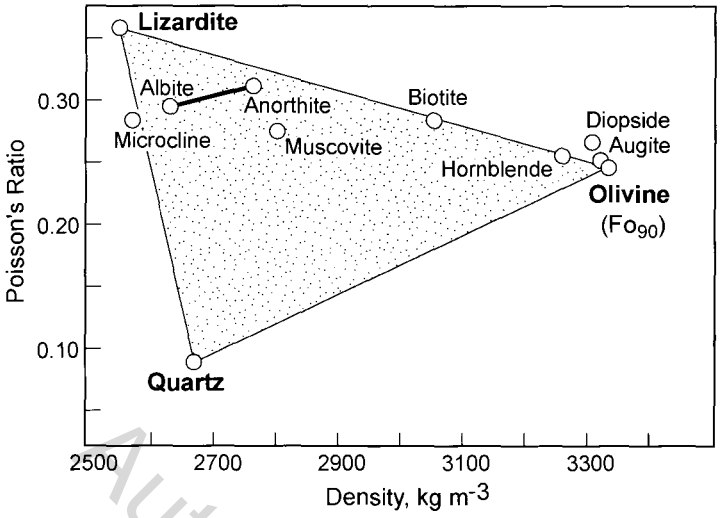

FIG. 2. Poisson's ratio versus density for common rock forming minerals (data from Christensen, 1996).

This simplifies many of the mathematical relationships between elastic moduli (e.g., the bulk modulus, Young's modulus, and Lame's constants), density, and velocities. For $\sigma = 0.25$, $Vp/Vs = \sqrt{3} = 1.732$.

Common rock types usually have Poisson's ratios which fall between 0.10 and 0.40 (Christensen, 1996). Poisson's ratios of lizardite-chrysotile serpentinites average 0.36 at 1 GPa. Plotting densities against Poisson's ratios for available data on common rock-forming minerals (Fig. 2) shows that most minerals fall within a triangular distribution bounded by quartz with a low density and low Poisson's ratio, olivine with a high density and intermediate Poisson's ratio, and serpentine (lizardite) with a low density and high Poisson's ratio. Changes in density and Poisson's ratio accompanying serpentinization follow the upper leg of the triangle in Figure 2.

Recent studies concerned with interpreting seismic velocities in regions of probable serpentinization have used the relationships shown in Figure 1 to estimate serpentine abundances in a variety of tectonic settings (e.g., Carlson and Miller, 1997; Bostock et al., 2002; Omori et al., 2002). Horen et al. (1996) concluded that new velocity-density measurements at atmospheric pressure on 6 serpentinized peridotites from the Xigaze ophiolite (Tibet) compare favorably with the data shown in Figure 1. More recently, Carlson and Miller (2003) corrected the velocities of Figure 1 for temperature and presented a figure showing the variations of P and S velocities, velocity ratio, and density with serpentinization at P-T conditions for upper mantle rocks above subducting plates.

New velocity-density plots are shown in Figure 3 using published ultramafic rock velocities and densities of Birch (1960), Simmons (1964), and Christensen (1966, 1971, 1972a, 1978), as well as unpublished data measured from a suite of partially serpentinized peridotites and dunites from Cypress Island, Washington state. Data were selected from rocks in which velocities were measured in three or more directions to a confining pressure of 1 GPa. Because most of the relatively unaltered rocks were dunites, the high-density data sets approximate velocities and densities of olivine. The low-density rocks of this data set were limited to specimens containing primarily lizardite and chrysotile serpentine. The velocities in Figure 3 have been corrected for temperature using the data of Christensen (1979) and Birch (1943). The temperature (200°C) and pressure (200 MPa) of Figure 3 are appropriate for oceanic lower crust and upper mantle.

Poisson's ratios, calculated from the least squares solutions in Figure 3, are shown in Figure 4. At appropriate pressures, the end member Poisson's ratios of Figure 4 fall within one standard deviation of average values of dunite and serpentinite given by Christensen (1996).

Deviations of individual data points in Figure 3 from the least squares solutions may arise from errors of measurement, anisotropy, differences in

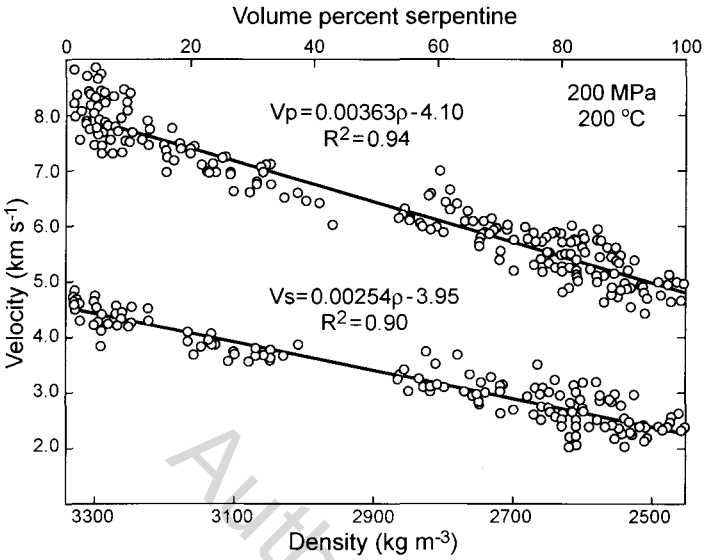

FIG. 3. Velocities at 200 MPa and 200°C versus volume percent lizardite-chrysotile serpentine and density.

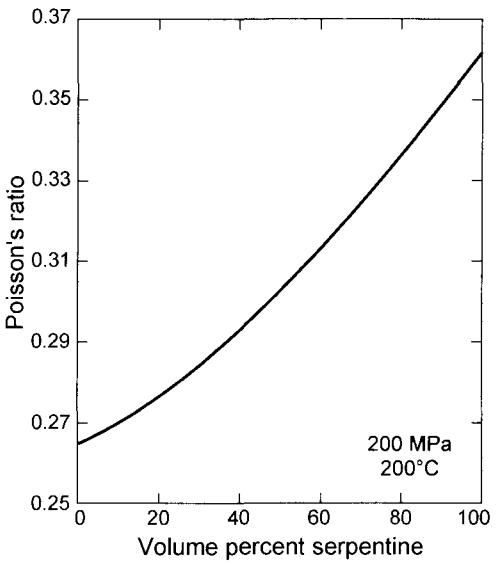

FIG. 4. Poisson's ratios calculated from the least squares solutions of Figure 3 versus volume percent lizardite-chrysotile serpentine.

mineral proportions in the parent peridotites and dunites, and the presence of other alteration products. Accuracies of the velocity measurements are estimated to be ±0.5% for Vp and ±1.0% for Vs. The high-density rocks possess significant velocity anisotropy originating from preferred mineral orientation, as discussed in the next section. On the other hand, petrographic examinations of the highly serpentinized rocks show mesh textures with no significant serpentine orientation. This observation is in agreement with those of O'Hanley (1966), who concluded that serpentine textures consist of fibers and plates with a myriad of orientations, and Horen et al. (1996), who observed low anisotropies (1% for Vp and 2% for Vs) in serpentinites.

Much of the data scatter in Figure 3, especially for the lower-density samples, is attributed to varying proportions of accessory minerals. In addition to olivine, the high-density samples may contain other minerals, the most common being pyroxene and chromite. As serpentinization progresses, various reaction products such as brucite, magnetite, chlorite, talc, tremolite, and magnesite may accompany the formation of serpentine. With the exception of magnetite, elastic constants have not been reported for these minerals. Measurements of the elastic properties of relatively pure crystalline aggregates, however, provide valuable information on average velocities and Poisson's ratios of single crystals. These measurements have certain advantages over single-crystal studies in that the elastic properties are easily measured at elevated pressures, and large gem-quality crystals are not necessary for the measurements. In addition, the study of randomly oriented aggregates eliminates uncertainties in

TABLE 1. Velocities (Vp, Vs) and Poisson's Ratios (σ) of Mineral Aggregates as a Function of Pressure (MPa)[1]

Mineral		Pressure (MPa) 200	400	600	800	1000	Reference[2]
Brucite	Vp	6.29	6.37	6.43	6.47	6.51	1
p = 2440	Vs	3.68	3.72	3.74	3.76	3.77	
	σ	0.24	0.24	0.24	0.25	0.25	
Magnesite	Vp	8.12	8.24	8.31	8.36	8.41	2
p = 2970	Vs	4.59	4.64	4.68	4.70	4.71	
	σ	0.27	0.27	0.27	0.27	0.27	
Chlorite	Vp	5.99	6.06	6.11	6.14	6.16	1
p = 3158	Vs	3.18	3.19	3.20	3.21	3.22	
	σ	0.30	0.31	0.31	0.31	0.31	
Magnetite	Vp	7.15	7.24	7.29	7.33	7.37	1
p = 5021	Vs	4.04	4.11	4.14	4.16	4.19	
	σ	0.27	0.26	0.26	0.26	0.26	
Lizardite	Vp	4.75	4.91	5.02	5.14	5.23	3
p = 2520	Vs	2.29	2.32	2.35	2.38	2.41	
	σ	0.35	0.36	0.36	0.37	0.37	
Antigorite	Vp	6.54	6.60	6.64	6.67	6.69	4
p = 2665	Vs	3.58	3.59	3.61	3.61	3.62	
	σ	0.29	0.29	0.29	0.29	0.29	
Orthopyroxene	Vp	7.67	7.74	7.80	7.85	7.96	5
p = 3285	Vs	4.51	4.54	4.56	4.57	4.59	
	σ	0.24	0.24	0.24	0.24	0.25	
Olivine	Vp	8.27	8.33	8.36	8.38	8.40	6
p = 3317	Vs	4.75	4.80	4.82	4.83	4.84	
	σ	0.25	0.25	0.25	0.25	0.25	

[1]Vp and Vs are in km/s, density (p) is in kg/m^3.
[2]1 = Christensen, unpubl.; 2 = Christensen, 1972b; 3 = Christensen, 1966; 4 = Christensen, 1978; 5 = Babuska, 1972; 6 = Christensen and Ramananantoandro, 1971.

calculations of elastic properties of crystalline aggregates from the elastic constants of component crystals (Birch, 1961, 1972).

Velocities and Poisson's ratios of several monomineralic aggregates determined to pressures of 1 GPa are summarized in Table 1. Previously unpublished data include measurements on brucite, chlorite, and magnetite. For comparison, similar data are given for olivine, orthopyroxene, lizardite, and antigorite. All of the data were averaged from velocities and densities of cores cut in multiple directions so as to minimize the effects of anisotropy. All samples are relatively pure, containing only small amounts of accessory minerals.

Comparisons of the properties of the various species of serpentine are important for meaningful interpretations of seismic data. Meaurements by Birch (1960) have shown that chrysotile has velocities similar to lizardite. Thus, variability in the proportions of these polymorphs does not appear to

significantly affect the seismic properties of serpentinites. Antigorite, on the other hand, has a much higher Vp and density (Birch, 1969) and a lower Poisson's ratio and higher Vs (Christensen, 1978) than lizardite. Previous studies have also found major differences in the mechanical properties of antigorite and lizardite. Antigorite has a greater ultimate strength, and the transition from ductile to brittle behavior of antigorite takes place at higher temperatures (Raleigh and Paterson, 1965; Raleigh, 1967). It is likely that these differences are related to the lower H_2O and and higher Si/Mg ratio of antigorite and the stronger bonding between layers in the crystal structure of antigorite (O'Hanley, 1996).

The orthopyroxene properties in Table 1 are for a bronzite composition (Babuska, 1972). The Mg end member enstatite has higher velocities and a lower Poisson's ratio (Christensen, 1996). A comparison of elastic properties of orthopyroxene with olivine (Table 1) shows that the addition of orthopyroxene to olivine-rich rocks with little serpentinization lowers velocities, density, and Poisson's ratio. The chlorite aggregate has velocities and a Poisson's ratio that fall between those of lizardite and antigorite. The presence of magnesite and/or magnetite in highly serpentinized rocks raises velocities and lowers Poisson's ratio. Brucite has a low Poisson's ratio and its velocities are significantly higher than lizardite and chlorite.

Seismic Anisotropy of Peridotite and Dunite

The first systematic measurements of compressional wave velocities in peridotites were made by Birch (1960). These measurements showed that anisotropy is a significant property of most dunites and peridotites. Since Birch's measurements were made at confining pressures to 1 GPa (equivalent to approximately 35 km depth), it was clear that the anisotropies originated from lattice-preferred orientations of olivine and pyroxene. At low pressures, it was found that oriented crack porosity produces anisotropy, but at high pressures, where crack porosity is eliminated, anisotropy is a measure of nonrandom mineral orientation.

The presence of anisotropy in partially serpentinized crustal and upper mantle regions complicates attempts to estimate serpentine and bound water contents from comparisons of seismic data with laboratory-measured velocities and Poisson's ratios. A large literature has been devoted to measuring and calculating seismic anisotropy in ultramafic rocks. Single-crystal olivine of appropriate mantle composition has a Vp anisotropy of 24%. Obviously this would be a value measured seismically only if a large portion of the mantle consisted of a single olivine crystal, an unlikely scenario. A common approach to estimate the magnitude of mantle anisotropy has been to average individual hand sample values calculated from petrofabric measurements of olivine orientations in thin sections (e.g., Ben Ismail and Mainprice, 1998). This approach does not take into account variability in the field orientations of rock foliations and thus gives high Vp and Vs anisotropies. More reliable anisotropies are obtained from determining the overall anisotropies of large ultramafic massifs from anisotropies determined from multiple field oriented samples. Using this procedure Christensen (2002) found maximum Vp and Vs wave anisotropies of 5.4% and 3%, respectively, for the Twin Sisters massif of Washington state, which consists of relatively unaltered dunite with an area of exposure of 75 km^3. Simple averages of individual hand samples give anisotropies nearly twice as great.

A second large surface exposure of mantle rocks ideal for anisotropy studies is the Permian Red Hills massif (Coleman, 1966; Coombs et al., 1976) located on the South Island of New Zealand. This is one of the largest and best exposed sections of relatively unaltered upper mantle peridotite in the world, with over 1 km of exposed vertical section and an outcrop area of approximately 110 km^2. The ultramafic rocks are in contact with Permian volcanics and a variety of sedimentary rocks, including sandstone, argillite, greywacke, and limestone. To the South, the massif is terminated by the Wairau fault, a branch of the Alpine fault. Numerous faults bound and crosscut the massif, and detailed mapping by Walcott (1969) has shown the presence of a major fold in its south-central portion (Fig. 5). The Motueka River follows the strike of layering and foliation, which defines a southward-plunging anticline. A swarm of basic dikes with uniform NNW strikes cuts the folded peridotite. The folding within the Red Hills massif originated at mantle temperatures high enough to produce ductile deformation of peridotite. Since the massif is part of a major ophiolite belt (Coombs et al., 1976) and appears to be relatively shallow upper oceanic mantle, because of associated crustal gabbro along its western margin, the folding likely developed at elevated temperatures near a ridge crest.

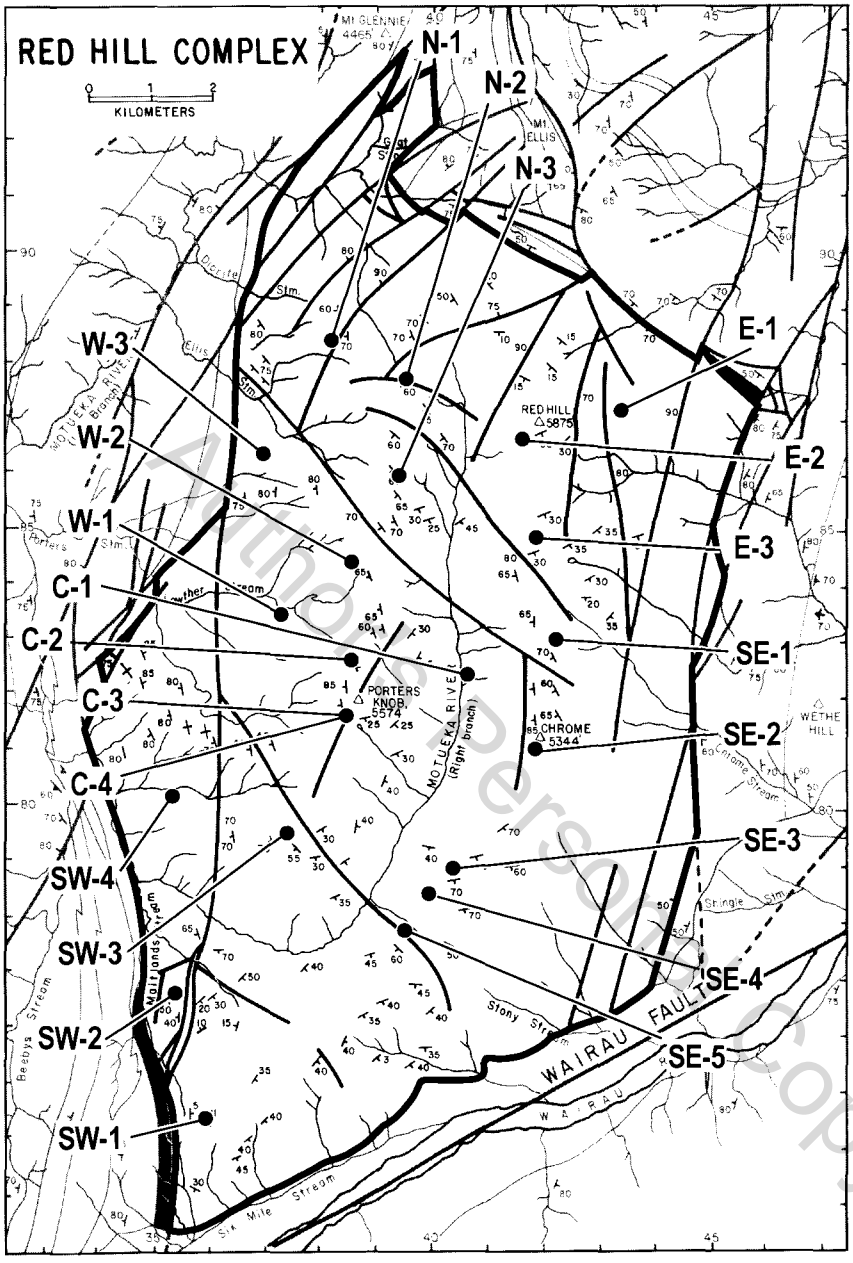

FIG. 5. Structure of the Red Hills massif (modified from Walcott, 1969) showing sample locations for petrofabric studies.

Twenty-two field-oriented peridotite samples, locations of which are given in Figure 5, were selected for petrofabric analyses using a five-axis universal stage. Thin sections were cut from each sample and orientations of the crystallographic axes of olivine and orthopyroxene grains were determined using the technique of Emmons (1943). Results of the petrofabric studies of olivine are presented in Figure 6 as lower hemisphere Kamb plots of the concentrations of crystallographic axes.

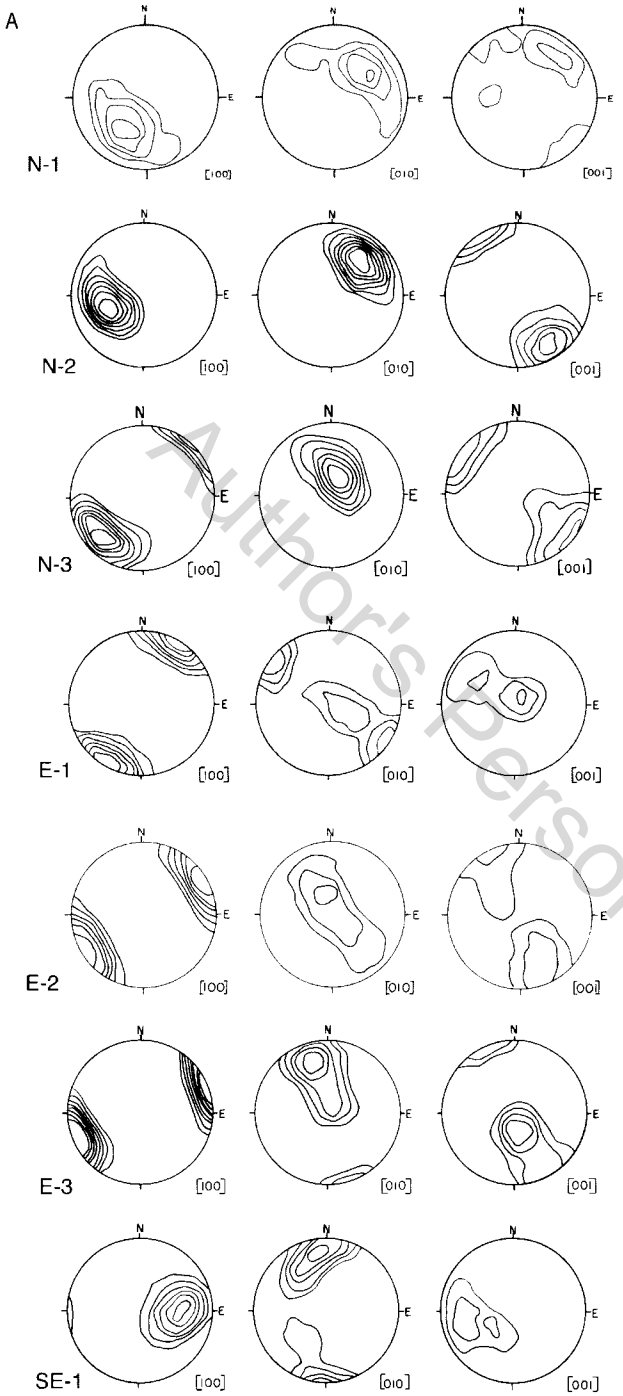

FIG. 6. Equal-area, lower hemisphere projections of [100], [010], and [001] axes of olivine. The projections are contoured in 2σ intervals with the lowest contour = 4σ. Sample locations are shown in Figure 5. Figure continues on following pages.

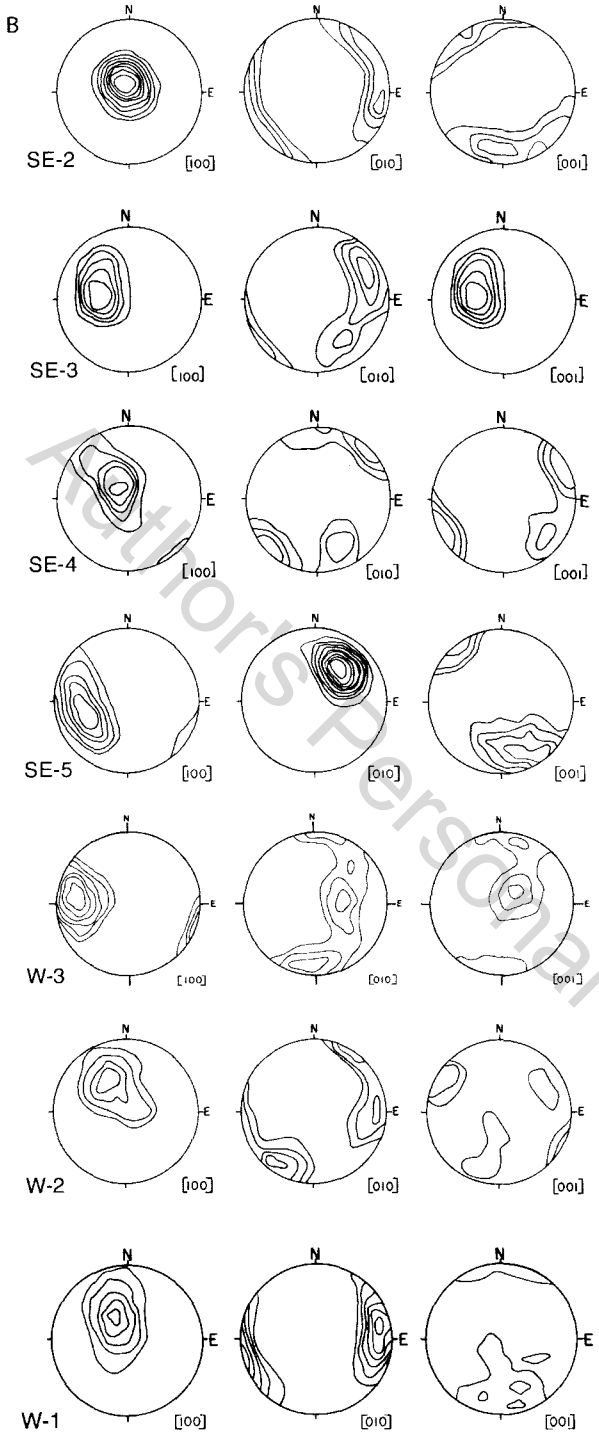

FIG. 6B.

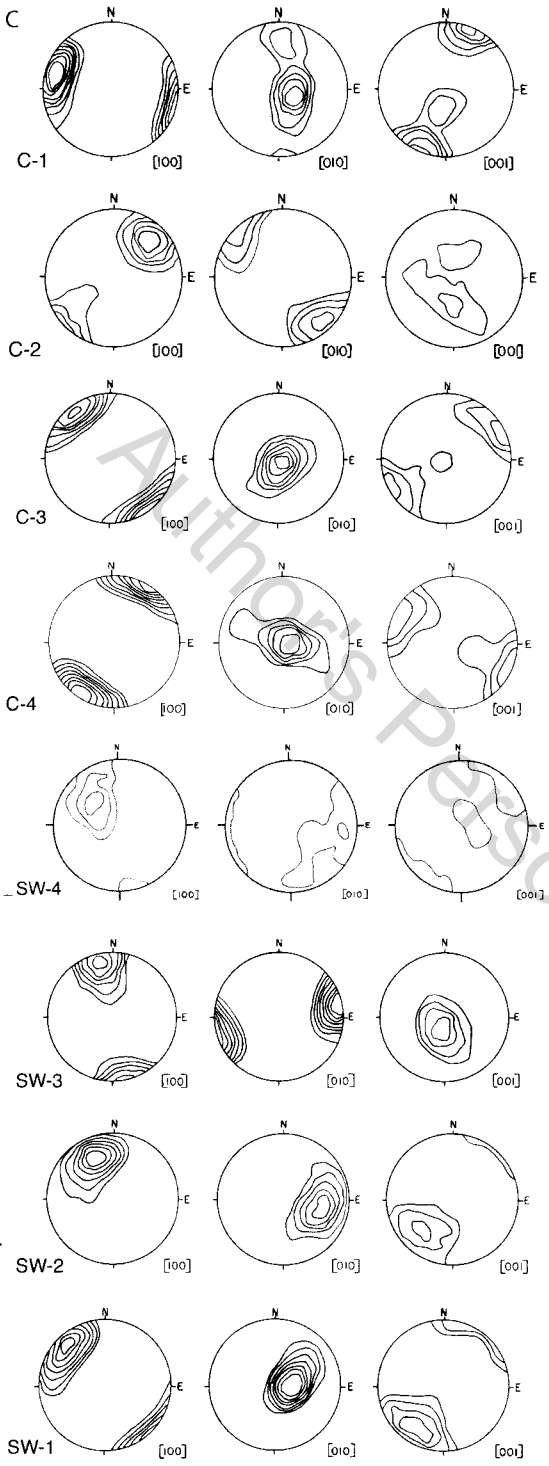

FIG. 6C.

Enstatite fabrics measured for 16 of the harzburgites show weak crystallographic orientations with enstatite *c* and *a* axes chiefly parallel to olivine *a* and *b* axes.

The olivine fabric diagrams show strong axial concentrations that typically relate to the layering and foliation mapped by Walcott (1969). Starting in the North, samples N-1, N-2, and N-3 show similar orientations of olivine axes with orthorhombic symmetries. Olivine *a* axes, which approximate mantle flow directions (Nicolas and Christensen, 1987), dip southwest at moderate angles and olivine *b* axes dip to the northeast. Both olivine *a* and *c* axes are roughly parallel to foliation that strikes NNW and dips southwest. Note that the fabrics and foliations continue across several faults, suggesting minimal displacements along these faults. To the east, samples E-1, E-2, and E-3 have olivine *a* axes concentrations trending NE-SW and horizontal, parallel to the strike of the foliation. Olivine *b* and *c* axes form partial girdles. This orientation changes toward the south, where olivine *a* axes first dip steeply east (SE-1), become vertical (SE-2), and then dip 35° to 65°W (SE-3, SE-4, SE-5).

Olivine *a* axes in the southwestern (SW-1, SW-2, SW-3, and SE-4) and western (W-1, W-2, and W-3) portions of the massif dip at shallow angles to the northwest. Fabric symmetry in the southwestern section is orthorhombic with olivine *b* axes concentrations dipping to the east, whereas samples collected along the western margin have *b* axes that form partial girdles and are horizontal in W-1 and W-2. Samples in the vicinity of Porter's Knob show a variety of axial orientations consistent with observations of Walcott (1969) of intersecting layered structures in this region.

This variability of olivine orientations within the Red Hills massif results in a relatively low overall seismic anisotropy compared to that of individual samples (Table 2). The seismic anisotropies were calculated at a confining pressure of 1 GPa and a temperature of 500°C, using a modified program of Crosson and Lin (1971). From the single-crystal elastic constants of olivine and enstatite, their temperature and pressure derivatives (Kumazawa and Anderson, 1969; Frisillo and Barsch, 1972), and the orientation data, the program calculates the contribution of each mineral grain in specified directions using the Cristoffel equation (Musgrave, 1970). Two S wave velocities, with perpendicular polarization directions and one P wave velocity are obtained for each specified propagation direction. These velocities are then contoured to show total anisotropy patterns. The S wave anisotropies in Table 2, defined as the velocity difference in the split shear waves expressed as a percentage of the mean shear wave velocity, are given for propagation directions parallel to maximum and minimum splitting. Shear wave delay times are also given for a 100 km thick mantle section.

Contoured anisotropy diagrams for the Red Hills massif, based on mineral orientations from the 22 sample locations shown in Figure 5, are given in Figure 7 as lower hemisphere projections. Field-oriented contoured diagrams are shown for P wave velocity (Vp), the fast S wave velocity (Vs1), S wave anisotropy, and shear wave splitting delay times for a 100 km thick mantle section.

Anisotropy of the Red Hills massif and average anisotropies of individual samples are compared in Table 3 with the Twin Sisters massif. These comparisons leave the impression that anisotropies of both ultramafic bodies are comparable. The Red Hills massif is slightly less anisotropic, which is clearly due to more variability in foliation orientations and related mineral fabrics, even though individual samples show greater anisotropies. Of interest, both bodies possess two directions of shear wave singularity, similar to optic axial directions of biaxial crystals in optical mineralogy. Individual Red Hills samples have on the average almost three times the overall P and S wave anisotropies of the massif (Table 3).

In Figure 8A, which takes into account anisotropy, Vp and Vs at 1 GPa and 500°C are plotted versus volume percent lizardite and antigorite. The 1 GPa serpentine velocities are from Table 1, and temperature corrections were applied to the data using the measurements of Birch (1943) and Christensen (1979). Velocities for the dunite end member have been calculated using the isotropic 1 GPa velocities of dunite in Table 1, corrected for temperature, and the average percentage anisotropies of the Red Hills and Twin Sisters massifs summarized in Table 3. It is assumed that anisotropy decreases linearly with increasing serpentinization. As was discussed earlier, most serpentine-bearing peridotites show random serpentine orientations.

Velocity ratios rather than Poisson's ratios are shown in Figure 8B, inasmuch as Poisson's ratios are defined only for isotropic solids. The dunite end member velocity ratios were averaged from velocities for the propagation directions producing maximum shear wave splitting in the Red Hills and Twin

TABLE 2. Red Hills Compressional Wave (Vp) Anisotropies, Shear Wave (Vs) Anisotropies, and Splitting Delay Times

Sample	Vp Anisotropy (%)	Maximum splitting direction Vs anisotropy (%)	Maximum splitting direction Delay time (s 100 km slab)	Minimum splitting direction Vs anisotropy (%)	Minimum splitting direction Delay time (s) 100 km slab
N-1	9.9	7.8	1.55	0.2	0.05
N-2	14.0	9.6	1.80	0.2	0.05
N-3	14.5	9.5	1.79	0.4	0.09
E-1	10.0	7.0	1.38	0.0	0.00
E-2	14.2	9.7	1.81	0.0	0.00
E-3	15.5	10.0	1.85	0.4	0.09
SE-1	12.3	8.3	1.64	0.2	0.05
SE-2	14.1	9.4	1.78	0.0	0.00
SE-3	11.5	8.0	1.58	0.2	0.05
SE-4	9.0	8.2	1.62	0.2	0.05
SE-5	13.1	10.1	1.87	0.1	0.02
SW-1	14.6	10.1	1.87	0.2	0.05
SW-2	11.5	8.0	1.58	0.2	0.05
SW-3	13.0	9.2	1.76	0.0	0.00
SW-4	6.0	4.5	0.97	0.0	0.00
W-1	11.6	8.4	1.65	0.0	0.00
W-2	10.6	7.6	1.50	0.0	0.00
W-3	11.1	7.9	1.57	0.1	0.02
C-1	14.6	10.7	1.97	0.0	0.00
C-2	10.7	8.4	1.65	0.2	0.05
C-3	13.1	9.4	1.78	0.2	0.05
C-4	15.5	10.5	1.95	0.2	0.05
Sample average	12.3	8.7	1.63	0.1	0.03
Massif	4.2	3.3	0.67	0.0	0.00

Sisters massifs. A Vp of 8.12 km/s, Vs1 of 4.81 km/s, and a Vs2 of 4.55 km/s gives velocity the ratios 1.785 and 1.688 used in Figure 8B. A larger velocity ratio range of 1.833 to 1.642 is obtained by combining the average maximum Vp of the two massifs with the average minimum Vs, and the average minimum Vp with the average maximum Vs.

Figure 8 illustrates several features that are important in estimating serpentine contents from seismic observations. First, antigorite has quite different velocities and velocity ratios than lizardite serpentinites. Thus, an understanding of the stability fields of these serpentine species is critical in applying laboratory results to the interpretation of seismic data. This will be addressed in the following section. Second, anisotropy must be taken into account before reasonable percentages of serpentine can be estimated from velocities and velocity ratios. This is especially important in regions containing relatively low percentages of serpentine. Also, velocity ratios are less diagnostic of antigorite serpentinization than lizardite serpentinization, because of the relatively low velocity ratio of antigorite.

Serpentine Contents of the Lower Oceanic Crust and Forearc Upper Mantle

Chrysotile and lizardite are structural varieties of serpentine with similar compositions and elastic properties, whereas antigorite differs in composition and elastic properties. Thus the stability fields of

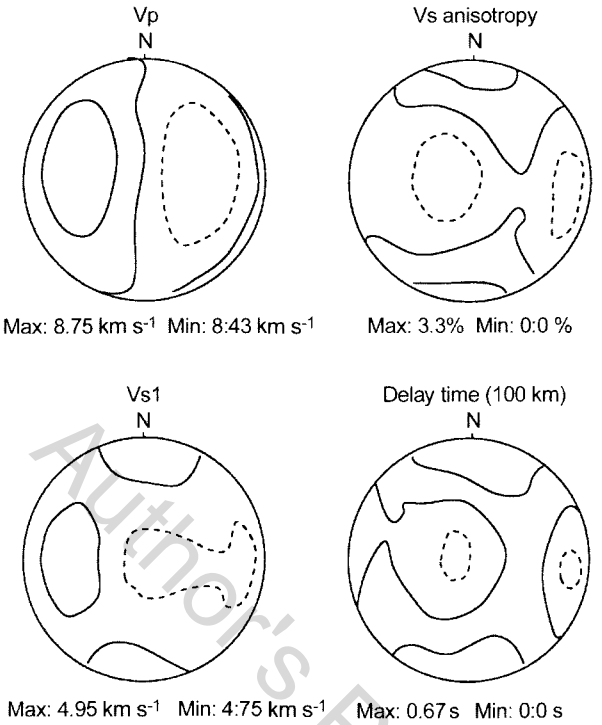

FIG. 7. Field-oriented Red Hills compressional wave velocity (Vp), shear wave (Vs) anisotropy, fast shear wave velocity (Vs1), and delay times for a 100 km slab. Contour intervals are 0.1 km/s for Vp, 0.05 km/s for Vs1, 1% for Vs anisotropy, and 0.2s for 100 km slab delay time. Minimum contours are shown as dashed lines.

TABLE 3. Anisotropy Comparisons of the Red Hills and Twin Sisters Massifs

Seismic property	Red Hills	Twin Sisters
Massif		
Vp anisotropy	4.2%	5.4%
Vs maximum anisotropy	3.3%	3.9%
Vs minimum anisotropy	0.0%	0.0%
Maximum delay time (100 km)	0.7sec	0.8 sec
Minimum delay time (100 km)	0.0sec	0.0 sec
Sample average		
Vp anisotropy	12.3%	9.8%
Vs maximum anisotropy	8.7%	7.6%
Vs minimum anisotropy	10.0%	0.3%
Maximum delay time (100 km)	1.6sec	1.5 sec
Minimum delay time (100 km)	0.0sec	0.1 sec

these species must be considered in the interpretation of seismic data from crustal and upper mantle regions with possible serpentinization (Coleman, 1971). Phase equilibria studies have shown that lizardite is stable below about 300°C, whereas only antigorite is stable above 300°C (Berman, 1988; O'Hanley, 1996; Evans, 2004). This is consistent with field observations documenting the presence of

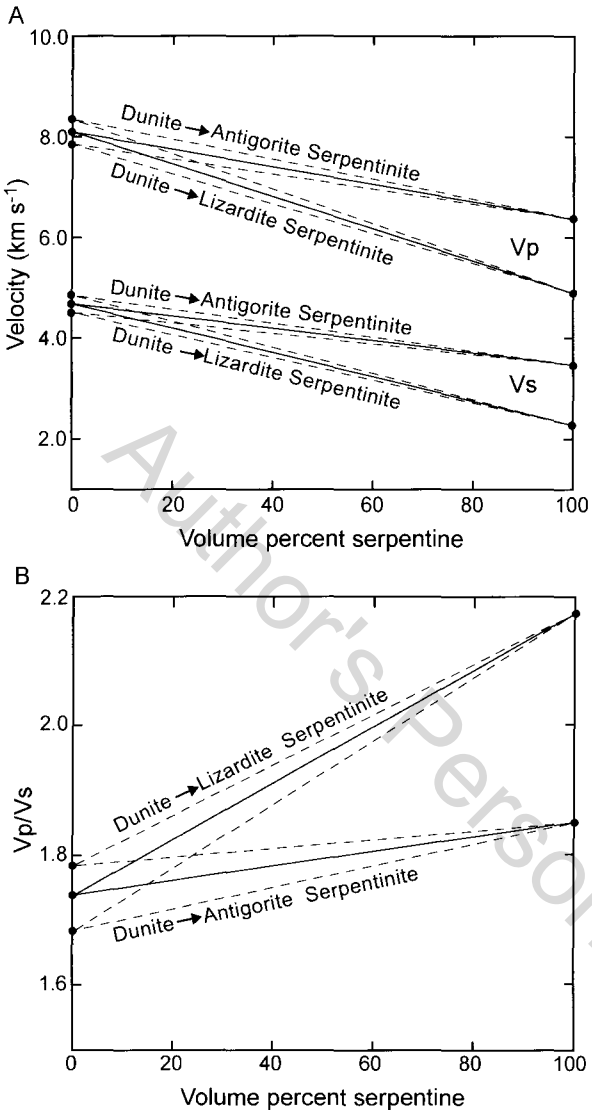

FIG. 8. Velocities and velocity ratios at 1GPa and 500°C versus percent serpentinization (data from Table 1). Dashed lines show possible scatter caused by anisotropy.

lizardite in subgreenschist-facies rocks and antigorite in greenschist- and amphibolite-facies assemblages. Evans (2004) has shown that chrysotile has no P-T stability field at all, although it occurs commonly in low-temperature serpentinites. The decomposition temperature of antigorite at upper mantle pressures is approximately 650°C (Ulmer and Trommsdorff, 1995; Wunder and Schreyer, 1997; Bromiley and Pawley, 2003).

The phase diagram of Evans (2004) for lizardite and antigorite is shown in Figure 9. Superimposed on this diagram are approximate P-T fields for two regions of possible widespread serpentinization, the lower oceanic crust and forearc upper mantle. Note that lizardite is stable in oceanic crustal environments, whereas antigorite is the stable serpentine in forearc upper mantle where temperatures are in the range of 350° to 600°C.

The Lower Oceanic Crust

The formation and abundance of serpentine in the oceanic crust have been controversial topics of marine geology for over four decades. Hess (1962) was the first to propose that the lower oceanic crust is composed of serpentine, formed by hydration of mantle peridotite. Serpentinization was originally proposed by Hess as an explanation for epeirogenic movements of the sea floor and in continental regions such as the Colorado Plateau, and later developed into a model to explain the formation of oceanic crust. Hess suggested that mantle peridotite hydrates near ocean ridge crests as it passes through the 500°C isotherm and spreads laterally to form the lower 5 km (layer 3) of the oceanic crust (Fig. 10). The newly formed serpentinite moves away from spreading centers, carrying with it upper oceanic crust consisting of basalt created at ridge crests and oceanic sediments.

A large number of papers have addressed this model. The major argument for an oceanic crust with abundant serpentine comes from dredging and drilling, which have recovered *in situ* serpentinite (e.g., Aumento and Loubat, 1971; Bonatti et al., 1974; Juteau et al., 1990). These oceanic serpentinites consist primarily of mesh-textured lizardite and chrysotile (O'Hanley, 1996). The degree of serpentinization is usually quite advanced, resulting in velocities much lower than typical lower oceanic crustal values of 6.7 to 7.0 km/s (e.g., Christensen, 1972a). Also, estimates of temperatures of serpentinization of oceanic serpentinites from oxygen isotope studies of serpentine-magnetite pairs fall below 170°C (Evans and Baltuck, 1988; Viti and Mellini, 1998). This suggests that serpentinization occurs at shallow crustal depths rather than at the 500°C isotherm proposed by Hess.

It is likely that much oceanic serpentinite is localized on fault escarpments associated with ridge axes and transform faults (Francis, 1981; White et al., 1984; Cannat et al., 1992). Thus oceanic crust formed at slow spreading ridges, where normal faulting is common, likely contains significantly higher amounts of serpentine than crust formed at fast spreading ridges (MacDonald, 1982). Ultraslow spreading ridges (Dick et al., 2003) may also prove to be major sources of oceanic crustal serpentinite.

The deepest drill hole in the oceanic crust, 504B, located in the eastern Pacific approximately 200 km south of the Costa Rica Rift, recovered metadiabase with layer 3 seismic velocities (Christensen et al., 1989; Salisbury et al., 1996). The stratigraphy at this site, consisting of volcanics underlain by sheeted dikes, is similar to upper and middle sections of many ophiolites, suggesting that the lowermost crust in this region is composed of metadiabase and possibly gabbro rather than serpentinized peridotite. The finding that many ophiolites have seismic profiles similar to that of the oceanic crust (Christensen, 1978) lends strong support to an ophiolite model of oceanic crustal composition (Coleman, 1977), which does not require major amounts of serpentinite in the lower crustal section.

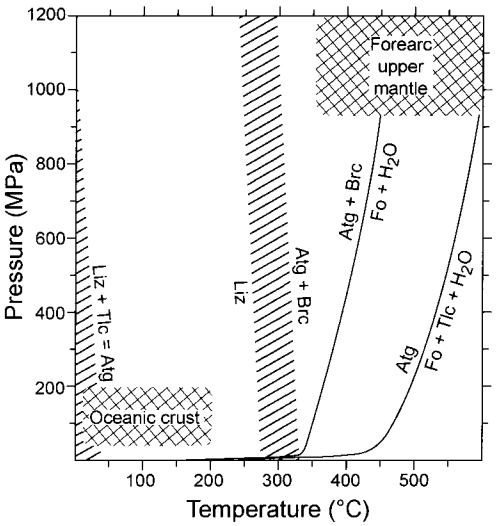

FIG. 9. Stability fields of serpentine minerals (from Evans, 2004) and P-T fields of normal lower oceanic crust and forearc upper mantle. Abbreviations: Liz = lizardite; Atg = antigorite; Tlc = talc; Brc = brucite; Fo = fosterite.

Until we core *in situ* lower crust in a variety of tectonic environments and with deeper penetration than that of 504B, our main source for evaluating serpentine abundances in the deep crust comes from careful juxtaposition of laboratory velocity data with marine seismic profiles. A key to the identification of large volumes of oceanic serpentinite are the high Poisson's ratios of lizardite/chrysotile–bearing rocks. This requires knowledge of crustal shear wave velocities, which at present is very limited. Christensen (1972a) compared Vp and Vs profiles of Helmberger and Morris (1970) located in the Pacific Ocean north of the Hawaiian Islands with the velocity data of Figure 1 and concluded that serpentinite is not a major constituent of the oceanic

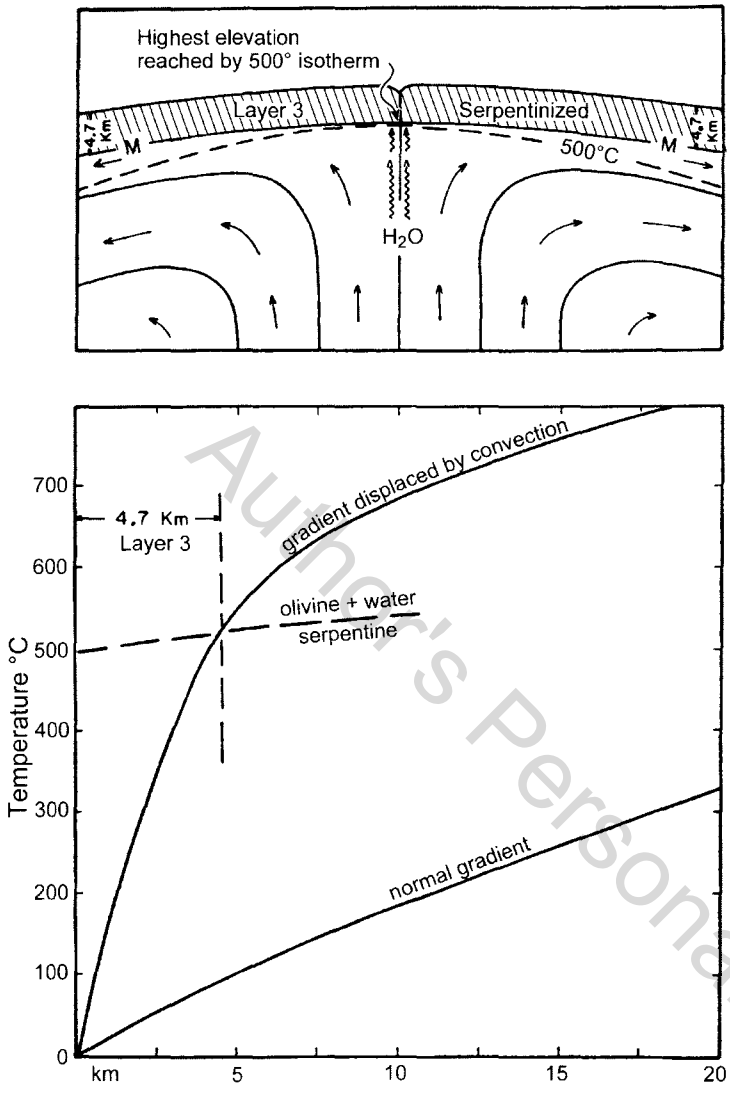

FIG. 10. A model (after Hess, 1962) to form serpentinized lower oceanic crust at ridge crests. Water from the mantle forms serpentinite above the 500°C isotherm.

crust in this region. More recent comparisons by Carlson and Miller (1997) of oceanic rock velocities with *in situ* velocities from the Atlantic crust also support a mafic model for the lower oceanic crust. This conclusion is based on comparisons of Atlantic profiles from the NAT (North Atlantic Transect) Study Group (1985), Minshull et al. (1991), and Morris et al. (1993) with laboratory velocities of oceanic diabase and gabbro and serpentinized peridotites (Fig. 11). The good agreement of the *in situ* seismic data with measured velocities in oceanic gabbros and diabases demonstrates that serpentinite is not likely a major constituent of the oceanic crust in these regions of the Atlantic. Quantitative estimates of partially serpentinized peridotite and gabbro abundances based on average rock elastic properties compared with these seismic profiles suggest that the average content of the ultramafic rocks in the Atlantic crust is less than 13% (Carlson, 2001). Clearly, it is essential in future marine seismic studies to obtain high quality Vp and Vs data in a variety of tectonic regions, so that we can

evaluate the abundance and distribution of serpentinite within the oceanic crust and better understand the physical and chemical processes that produce oceanic crust.

Forearc Upper Mantle

New seismic data as well as petrologic modeling have renewed interest in understanding geologic processes active in forearc upper mantle. Wilson (1954) was one of the first to suggest that water-rich solutions were generated at Benioff zones, and on their way up they react with overlying mantle. In subsequent seismic studies it was found that the wedge of mantle overlying subduction zones displays unusual seismic properties at shallow depths. In particular it was observed that Vp and Vs are significantly lower than normal as well as strongly attenuated (Molnar and Oliver, 1969; Barazangi and Isacks, 1971). These observations were accompanied by a cascade of papers emphasizing the importance of the role of water liberated by dehydration of the oceanic crust and carried upward into the mantle wedge (e.g., Oxburgh and Turcotte, 1968; Ringwood, 1969; Wyllie, 1971).

Seismic tomographic images of Vp and Vs have provided new detailed pictures of subduction zones and upper mantle slabs. Much ingenuity and intuition have gone into the construction of these structural and velocity cross sections. An example of a Vs tomograpic image and its structural interpretation for a profile extending from the coast through central Oregon is shown in Figure 12 (Bostock et al., 2002). In this figure, Vs perturbations across the continental Moho, near 32 km depth, show a Vs increase from relatively low velocity continental crust to high velocity mantle along the eastern portion of the profile. Moving to the west, there is a region of no velocity contrast and between approximately 122.6 and 123.3°W the continental Moho has an inverted velocity contrast, in which the lower-crustal rocks possess higher velocities than the underlying forearc mantle. This region of low-velocity upper mantle has been interpreted by Bostock et al. (2002) as having undergone pervasive serpentinization resulting from the upward migration of slab-released water. Similar observations of anomalous upper mantle forearc velocities (e.g., Peacock and Hyndman, 1999; Kamiya and Kobayashi, 2000) and associated high Poisson's ratios (Graeber and Asch, 1999; Omori et al., 2002) appear to support the ubiquitous presence of serpentinite in forearc upper mantle.

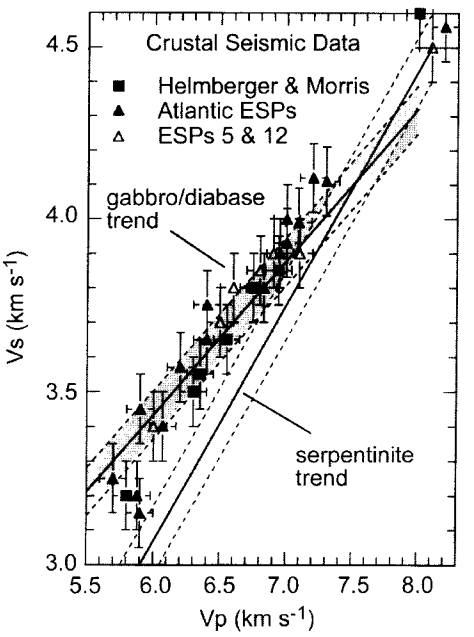

FIG. 11. Comparisons of oceanic crustal seismic velocities with linear best fits to laboratory measured velocities of oceanic gabbro/diabase and partially serpentinized peridotite suites. The solid lines are least square fits to the laboratory data and the dashed lines indicate RMS errors (from Carlson and Miller, 1997). Note the agreement of the field data with the gabbro/diabase velocities.

Using earthquake tomography and controlled-source seismic surveys, Brocher et al. (2003) have demonstrated that low-velocity forearc upper mantle can be traced from the southeastern end of Vancouver Island southward to the southern edge of the Klamath terrane of northern California. Moho reflections from the forearc upper mantle are not observed along this band of low-velocity upper mantle, which is interpreted to originate from partial serpentinization.

While some of these studies (e.g., Bostock et al., 2002; Omori et al., 2002) recognize that antigorite is the stable serpentine at forearc wedge P-T conditions (Fig. 9), interpretations of serpentine contents have been based on the elastic properties of olivine-lizardite-chrysotile assemblages rather than olivine-antigorite assemblages, which have higher velocities and lower velocity ratios (Table 1, Fig. 8). Upper-mantle forearc compressional wave veloci-

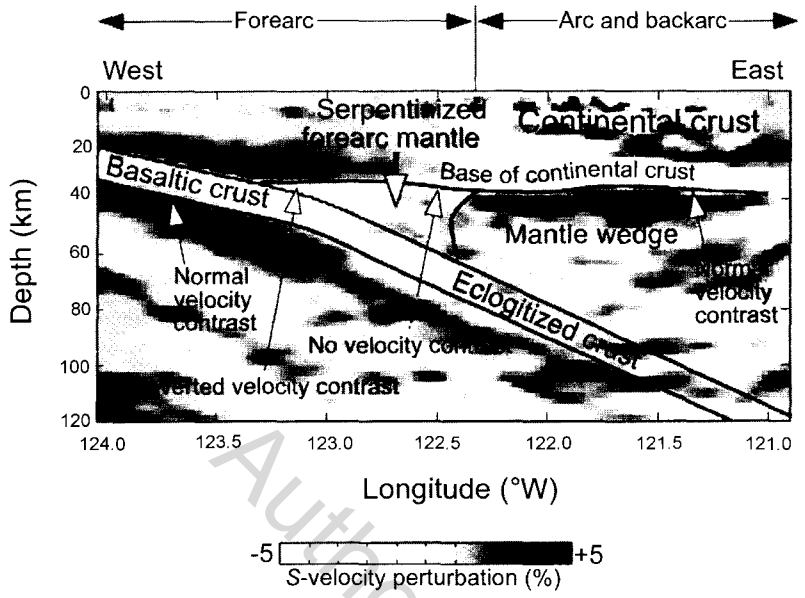

FIG. 12. Shear wave velocity model of Cascadia subduction zone in central Oregon (modified from Bostock et al., 2002 and Brocher et al., 2003). The seismic properties of the low velocity forearc mantle region are unlikely to have originated from serpentinization (see text).

ties, where temperatures are believed to be low enough for antigorite to be stable, tend to be between 6.7 to 7.6 km/s (Kamiya and Kobayashi; 2000; Seno et al., 2001; Brocher et al., 2003). Superimposing this velocity range on the dunite-antigorite Vp curve of Figure 8, we obtain volume percentages of antigorite of 20 to 86%, allowing for velocity uncertainties due to possible anisotropy. Corresponding velocity ratios fall between 1.72 and 1.84, equivalent to Poisson's ratios of 0.25 and 0.29. The limited observed Poisson's ratios for forearc upper mantle slabs are generally higher, and values of 0.30 in the Kanto area of NE Japan (Omori et al., 2002) and 0.34 beneath central Japan (Kamiya and Kobayashi, 2000) are higher than for pure antigorite (Table 1). Thus, the physical interpretation of forearc upper mantle velocities is still uncertain. Perhaps serpentine is not abundant and other factors are lowering velocities and increasing Poisson's ratios in these mantle regions.

The presence of antigorite instead of unaltered peridotite in forearc wedge mantle lowers velocities and increases Poisson's ratios. However, these differences are relatively small compared to changes produced by lizardite-chrysotile alteration of peridotite. As was discussed above, other processes are likely important in these regions. Several possibilities come to mind that affect elastic properties such that peridotite velocities decrease and Poisson's ratios increase. High temperature, which lowers velocities, can be eliminated because thermal modeling of these regions results in low temperatures. Also, Poisson's ratio does not vary significantly with temperature (Christensen, 1996).

Chlorite, a common product of hydrothermal alteration of pyroxenes, amphiboles, and biotite in igneous rocks and a mineral stable in metaperidotite under greenschist- and amphibolite-facies conditions (Trommsdorff and Evans, 1972), has lower velocities than unaltered peridotite and a high Poisson's ratio (Table 1). We would expect to find chlorite in metamorphosed mantle slabs that are relatively undepleted (lherzolitic). The Al content of the fertile peridotite will control the upper limit of the amount of chlorite formed from the peridotite. However, if gabbro and/or mafic granulite are interlayered with the mantle peridotite, the generation of larger amounts of chlorite is likely. Of significance, the occurrence of chlorite with antigorite seems to be quite common (O'Hanley, 1996). The elastic properties of tremolite and talc, which characteristically are associated with antigorite and chlorite in

metamorphosed ultramafic rocks, have not been measured. Hornblende has a low Poisson's ratio (Christensen, 1996), thus the presence of tremolite in mantle forearc slabs probably decreases Poisson's ratio.

Tomographic studies have not addressed seismic anisotropies of the subducting slab and overlying forearc mantle peridotites. Velocity anisotropies in these regions could account for significant proportions of velocity deviations reported in seismic tomography cross sections. For example, the total Vs perturbation of the velocity model shown in Figure 12 is 10%, whereas the average Vs anisotropies of the Twin Sisters and Red Hills massifs are 3.9 and 3.3%, respectively (Table 3). Further complications arise from shear wave splitting, which occurs for most upper mantle propagation directions (Fig. 7). Significant hydration will, however, lower anisotropies as illustrated in Figure 8. It seems likely that anisotropy could produce low anomalous velocities and high Poisson's ratios in a tomographic profile, but at the same time there is an equal probability of obtaining high velocities and low Poisson's ratios.

A likely cause of low upper mantle velocities in regions being penetrated by significant quantities of aqueous fluid given off by underlying continuous dehydration is high pore pressure. It is well known that many rock physical properties depend not only on their mineralogies but also on the nature of contained pore fluids (e.g., Hubbert and Rubey, 1959; Raleigh, 1971; Todd and Simmons, 1972). Of particular significance for seismology is the pressure of the interstitial pore fluid. Most studies of the influence of pore pressure on velocities have focused on sedimentary rocks; however, a few measurements have been made on low porosity crystalline rocks (e.g., Todd and Simmons, 1972; Christensen, 1989). To a first approximation, pore pressure and confining pressure have opposite, but roughly equal, effects on velocities. That is, a decrease in velocity produced by an increase in pore pressure is similar to the increase in velocity produced by an equivalent increase in confining pressure. Experimental studies have found, however, that for some crystalline rocks a pore pressure change does not entirely cancel changes in velocities produced by an equal confining pressure change. Also, the magnitudes of velocity changes resulting from a given change in pore pressure increase with increasing porosity. Fluids rising through an upper mantle slab are likely to have pore pressures close to lithostatic. Measurements by Christensen (1989) on a relatively high porosity (3.9%) lherzolite xenolith from Kilbourne Hole, New Mexico show that at a confining pressure of 150 MPa, an increase of pore pressure from atmospheric to 85% of confining pressure lowers Vp by 9% and Vs by 26%, and increases Poisson's ratio from 0.27 to 0.36. Comparisons of these measurements with similar data from lower-porosity granite and andesite indicate that the magnitudes of these changes will likely be less for lower-porosity peridotites; however, the effects of pore pressure on velocities and Poisson's ratio will remain significant.

It is likely that the observed seismic properties of mantle forearc wedges are products of a variety of mineralogies and processes. The values of velocities and Poisson's ratios obtained for a given region may prove to be locally varying averages for anisotropic peridotite, with various hydrous alteration products and variable pore pressures. This is analogous to velocities of a rock, which to a first approximation are averages of the velocities of its individual minerals, their proportions, and even their anisotropies and lattice orientations as well as the abundance and pressures of pore fluids.

Conclusions

Experimental data on the elastic properties of peridotites and serpentinites provide valuable information for the interpretation of seismic studies of crustal and upper mantle velocity structure. Previously measured velocities in ultramafic rocks, ranging from unaltered peridotite to serpentinite, combined with additional unpublished data, confirm earlier findings of velocity-density relationships where the principal serpentine minerals are lizardite and chrysotile. Antigorite, a serpentine with a higher P-T stability field than lizardite, has higher velocities and a lower Poisson's ratio.

Anisotropy, an important property of ultramafic rocks, decreases with increasing serpentinization. Reliable values of upper mantle Vp and Vs anisotropies require careful analyses of multiple field-oriented samples from large, well-exposed ultramafic massifs. Average Vp anisotropy of the Red Hills (New Zealand) and the Twin Sisters (Washington state) massifs is 4.8%. Average maximum Vs splitting produces a delay time of 0.8 sec for 100 km of propagation. Both massifs show two directions of shear wave singularity.

A model of world-wide lower oceanic crust consisting of partially serpentinized peridotite is most

certainly wrong. Analyses of combined Vp and Vs data in the Atlantic and Pacific oceans compare well with laboratory velocities and velocity ratios of oceanic metadiabase and gabbro. Velocity ratios and related Poisson's ratios of partially serpentinized peridotite are higher than observed values in these "normal" crustal regions. There appears, however, to be localized serpentinization along transform faults, ridge-parallel faults, and crust formed at ultraslow ridges.

The present analysis indicates that the presence of antigorite alone is not adequate to explain the anomalous seismic properties of many mantle forearc wedges. What then is responsible for the low velocities and high Poisson's ratios of these regions? There are at least four possibilities: (1) chlorite, perhaps with antigorite, has formed by metamorphic processes; (2) anisotropy, which has not been taken into account in the data analyses, is responsible for anomalous velocities in some regions; (3) pore fluids rising through the mantle slab are at pressures approaching lithostatic; and (4) what seems most likely, all of the above.

Acknowledgments

This paper is presented in honor of Bob Coleman, whose many stimulating papers on serpentinites and related rocks are in large part responsible for my interest in ultramafic rocks. Bob has been a great friend for many years. Bernard Evans and Walter Mooney provided valuable comments on the manuscript.

REFERENCES

Aumento, F., and Loubat, H., 1971, The Mid-Atlantic ridge near 45°N, serpentinized ultramafic rocks: Canadian Journal of Earth Science, v. 8, p. 631–663.

Babuska, V., 1972, Elastic and anisotropy of dunite and bronzitite: Journal of Geophysical Research, v. 77, p. 6955–6965.

Barazangi, M., and Isacks, B., 1971, Lateral variation of seismic-wave attenuation in the upper mantle above the inclined earthquake zone of the Tonga island arc: Deep Anomaly in the upper mantle: Journal of Geophysical Research, v. 76, p. 8493–8516.

Ben Ismail, W., and Mainprice, D., 1998, An olivine fabric database: An overview of upper mantle fabrics and seismic anisotropy: Tectonophysics, v. 296, p. 145–157.

Berman, R. G., 1988, Internally consistent thermodynamic data for minerals in the system Na_2O-K_2O-CaO-MgO-FeO-Fe_2O_3-Al_2O_3-SiO_3-TiO_2-H_2O-CO_2: Journal of Petrology, v. 29, p. 445–523.

Birch, F., 1943, Elasticity of igneous rocks at high temperatures and pressures: Geological Society of America Bulletin, v. 54, p. 263–286.

_____, 1960, The velocity of compressional waves in rocks to 10 kilobars, part 1: Journal of Geophysical Research, v. 65, p. 1083–1102.

_____, 1961, The velocity of compressional waves in rocks to 10 kilobars, part 2: Journal of Geophysical Research, v. 66, p. 2199–2224.

_____, 1969, Density and composition of the upper mantle: First approximation as an olivine layer, *in* Hart, P. J., ed., The earth's crust and upper mantle: American Geophysical Union Monograph 13, p. 119–140.

_____, 1972, Numerical experiments on the velocities in aggregates of olivine: Journal of Geophysical Research, v. 77, p. 6385–6391.

Bonatti, E., Emiliani, C., Ferrara, G., Honnorez, J., and Rydell, H., 1974, Ultramafic carbonate breccias from the equatorial Mid-Atlantic Ridge: Marine Geology, v. 16, p. 83–102.

Bostock, M. G., Hyndman, R. D., Rondenay, S., and Peacock, S. M., 2002, An inverted continental Moho and serpentinization of the forearc mantle: Nature, v. 417, p. 536–538.

Brocher, T. M., Parsons, T., Trehu, A. M., Snelson, C. M., and Fisher, M. A., 2003, Seismic evidence for widespread serpentinized forearc upper mantle along the Cascadia margin: Geology, v. 31, p. 267–270.

Bromiley, G. D., and Pawley, A. R., 2003, The stability of antigorite in the systems MgO-SiO_2-H_2O(MSH) and MgO-Al_2O_3-SiO_2-H_2O (MASH): The effects of Al^3 substitution on high-pressure stability: American Mineralogist, v. 28, p. 99–108.

Buddington, A. F., 1943, Some petrological concepts and the interior of the Earth: American Mineralogist, v. 28, p. 119–140.

Cannat, M., Bideau, D., and Bougault, H., 1992, Serpentinized peridotites and gabbros in the Mid-Atlantic Ridge axial valley at 15°37'N and 16°52'N: Earth and Planetary Science Letters, v. 109, p. 87–106.

Carlson, R. L., 2001, The abundance of ultramafic rocks in the Atlantic Ocean Crust: Geophysical Journal International, v. 144, p. 37–48.

Carlson, R. L., and Miller, D. J., 1997, A new assessment of the abundance of serpentinite in the oceanic crust: Geophysical Research Letters, v. 24, p. 457–460.

_____, 2003, Mantle wedge water contents estimated from seismic velocities in partially serpentinized peridotites: Geophysical Research Letters, v. 30, no. 5, p. 1250 [doi:10.1029/2002GL016600].

Christensen, N. I., 1966, Elasticity of ultrabasic rocks: Journal of Geophysical Research, v. 71, p. 5921–5931.

_____, 1971, Fabric, seismic anisotropy, and tectonic history of the Twin Sisters Dunite, Washington:

Geological Society of America Bulletin, v. 82, p. 1681–1694.

_____, 1972a, The abundance of serpentinites in the oceanic crust: The Journal of Geology, v. 80, p. 709–719.

_____, 1972b, Elastic properties of polycrystalline magnesium, iron, and manganese carbonates to 10 kilobars: Journal of Geophysical Research, v. 77, p. 369–374.

_____, 1978, Ophiolites, seismic velocities and oceanic crustal structure: Tectonophysics, v. 47, p. 131–157.

_____, 1979, Compressional wave velocities in rocks at high temperatures and pressures, critical thermal gradients, and crustal low velocity zones: Journal of Geophysical Research, v. 84 , p. 6849–6857.

_____, 1989, Pore pressure, seismic velocities, and crustal structure, *in* Pakiser, L. C., and Mooney, W. D., Geophysical framework of the continental United States: Geological Society of America Memoir 172, p. 783–798.

_____, 1996, Poisson's ratio and crustal seismology: Journal of Geophysical Research, v. 101, p. 3139–3156.

_____, 2002, Continental mantle seismic anisotropy: A new look at the Twin Sisters massif: Tectonophysics, v. 355, p. 163–170.

Christensen, N. I., and Ramananantoandro, R., 1971, Elastic moduli and anisotropy of dunite to 10 kilobars: Journal of Geophysical Research, v. 76, p. 4003–4010.

Christensen, N. I., Wepfer, W. W., and Baud, R. D., 1989, Seismic properties of sheeted dikes from Hole 504B, ODP Leg 111: Proceedings of the Ocean Drilling Program, Scientific Results, v. 111, p. 171–176.

Coleman, R. G., 1966, New Zealand serpentinites and associated metasomatic rocks: Wellington, NZ, New Zealand Department of Scientific and Industrial Research, New Zealand Geology Survey Bulletin 76, Wellington, 102 p.

_____, 1971, Petrologic and geophysical nature of serpentinites: Geological Society of America Bulletin, v. 82, p. 918–987.

_____, 1977, Ophiolites: Berlin, Germany, Springer-Verlag, 329 p.

Coombs, D. S., Landis, C. A., Sinton, J. M., Norris, R. J., Borns, D. J., and Craw, D., 1976, The Dun Mountain ophiolite belt, New Zealand, its tectonic setting, constitution, and origin, with special reference to the southern portion: American Journal of Science, v. 276, p. 561–603.

Crosson, R. S., and Lin, J. W., 1971, Voigt and Reuss predictions of anisotropic elasticity of dunite: Journal of Geophysical Research, v. 76, p. 570–578.

Dick, H. J. B., Lin, J., and Schouten, H., 2003, An ultraslow-spreading class of ocean ridge: Nature, v. 426, p. 405–412.

Emmons, R. C., 1943, The universal stage: Geological Society of America Memoir , v. 8, 205 p.

Evans, B. W., 2004, The serpentine multisystem revisited: Chrysotite is metastable: International Geology Review, v. 46, p. 479–506.

Evans, C. A., and Baltuck, M., 1988, Low-temperature alterations of peridotite, Hole 637A, *in* Bolillot, G. and Winterer, E. L., eds., Proceedings of the Ocean Drilling Program: College Station, TX, Scientific Results, v. 103, p. 235–239.

Francis, T. J. G., 1981, Serpentinization faults and their role in the tectonics of slow spreading ridges: Journal of Geophysical Research, v. 86, p. 11616–11622.

Frisillo, A. L., and Barsch, G. R., 1972, Measurements of single-crystal elastic constants of bronzite as a function of pressure and temperature: Journal of Geophysical Research, v. 77, p. 6360–6384.

Graeber, F. M., and Asch, G., 1999, Three-dimensional models of P wave velocity and P-to-S velocity ratio in the southern central Andes by simultaneous inversion of local earthquake data: Journal of Geophysical Research, v. 104, p. 20,237–20,256.

Helmberger, D. V. and Morris, G. B., 1970, A travel time and amplitude interpretation of a marine refraction profile: Transformed shear waves: Bulletin of the Seismological Society of America, v. 60, p. 593–600.

Hess, H. H., 1959, The AMSOC hole to the Earth's mantle: American Geophysical Union Transactions, v. 40, p. 340–345.

_____, 1962, History of ocean basins, *in* Engel, A. E. J., James, H. L., and Leonard, B. F., eds., Petrologic studies, Buddington volume: Boulder, CO, Geologic Society of America, p. 599–620.

Horen, H., Zamora, M., Dubuisson, G., 1996, Seismic wave velocities and anisotropy in serpentinized peridotites from Xigaze ophiolite: Abundance of serpentine in slow spreading ridge: Geophysical Research Letters, v. 23, p. 9–12.

Hubbert, M. K., and Rubey, W. W., 1959, Role of fluid pressure in mechanics of overthrust faulting: Geological Society of America Bulletin, v. 70, p. 115–166.

Juteau, T., Cannat, M., and Lagabrielle, Y., 1990, Serpentinized peridotites in the upper oceanic crust away from transition zones: Proceedings of the Ocean Drilling Program, Scientific Results, v. 106/109, p. 303–308.

Kamiya, S., and Kobayashi, Y., 2000, Seismological evidence for the existence of serpentinized wedge mantle: Geophysical Research Letters, v. 27, p. 819–822.

Kumazawa, M., and Anderson, O. L., 1969, Elastic moduli, pressure derivatives, and temperature derivatives of single-crystal olivine and single-crystal forsterite: Journal of Geophysical Research, v. 74, p. 5961–5972.

MacDonald, K. C., 1982, Mid-ocean ridges: Fine scale tectonic, volcanic and hydrothermal processes within the plate boundary zone: Annual Reviews of Earth and Planetary Sciences, v. 10, p. 155–190.

Minshull, T. A., White, R. S., Mutter, J. C., Buhl, P., Detrick, R. S., Williams, C. A., and Morris, E., 1991,

Crustal structure at the Blake Spur fracture zone from expanding spread profiles: Journal of Geophysical Research, v. 96, p. 9955–9984.

Molnar, P., and Oliver, J., 1969, Lateral variations of attenuation in the upper mantle and discontinuities in the lithosphere: Journal of Geophysical Research, v. 74, p. 2648–2682.

Morris, E., Detrick, R., Minshull, T. A., Mutter, J. C., White, R. S., Su, W., and Buhl, P., 1993, Seismic structure of ocean crust in the western north Atlantic: Journal of Geophysical Research, v. 98, p. 13879–13903.

Musgrave, M. J. P., 1970, Crystal acoustics: San Francisco, CA, Holden-Day, 288 p.

NAT Study Group, 1985, North Atlantic Transect: A wide-aperture, two-ship multichannel seismic investigation of the oceanic crust: Journal of Geophysical Research, v. 90, p. 10,321–10,341.

Nicolas, A., and Christensen, N. I., 1987, Formation of anisotropy in upper mantle peridotites; a review, *in* Fuchs, K., and Froidevaux, C., eds., Composition, structure, and dynamics of the lithosphere-asthenosphere system: American Geophysical Union, Geodynamics Series, v. 16, p. 111–123.

O'Hanley, D. S., 1996, Serpentinites: Records of tectonic and petrologic history: New York, NY, Oxford University Press, 277 p.

Omori, S., Kamiya, S., Maruyama, S., and Zhao, D., 2002, Morphology of the intraslab seismic zone and devolatilization phase equilibria of the subducting slab peridotites: Bulletin of the Earthquake Research Institute, v. 76, p. 455–478.

Oxburgh, E. R., and Turcotte, D. L., 1968, Mid-ocean ridges and geotherm distribution during mantle convection: Journal of Geophysical Research, v. 73, p. 2943–2661.

Peacock, S. M., and Hyndman, R. D., 1999, Hydrous minerals in the mantle wedge and the maximum depth of subduction thrust earthquakes: Geophysical Research Letters, v. 26, p. 2517–2520.

Raleigh, C. B., 1967, Tectonic implications of serpentine weakening: Geophysical Journal of the Royal Astronomical Society, v. 14, p. 113–118.

_____, 1971, Earthquake control of Rangely, Colorado: EOS (Transactions of the American Geophysical Union), v. 52, p. 344.

Raleigh, C. B., and Paterson, M. S., 1965, Experimental deformation of serpentine and its tectonic implications: Journal of Geophysical Research, v. 70, p. 3965–3985.

Ringwood, A. E., 1969, Composition and evolution of the upper mantle, *in* The Earth's crust and upper mantle: American Geophysical Union Geophysical Monograph 13, p. 1–17.

Salisbury, M. H., Christensen, N. I., and Wilkens, R. H., 1996, Nature of the Layer 2/3 transition from a comparison of laboratory and logging velocities and petrology at the base of Hole 504B: Proceedings of the Ocean Drilling Program, Scientific Results, v. 148, p. 409–414.

Seno, T., Zhao, D., Kobayashi, Y., and Nakamura, M., 2001, Dehydration of serpentinized slab mantle: Seismic evidence from southwest Japan: Earth, Planets, and Space, v. 53, p. 861–871.

Simmons, G., 1964, The velocity of shear waves in rocks to 10 kilobars, 1: Journal ofGeophysical Research, v. 69, p. 1123–1130.

Todd, T., and Simmons, G., 1972, Effect of pore pressure on the velocity of compressional waves in low-porosity rocks: Journal of Geophysical Research, v. 77, p.3731–3743.

Trommsdorff, V., and Evans, B. W., 1972, Alpine metamorphism of peridotitic rocks: Scheizerische Mineralogische und Petrographische Mitteilungen, v. 54, p. 333–352.

Ulmer, P., and Trommsdorff, V., 1995, Serpentine stability to mantle depths and subduction-related magmatism: Science, v. 268, 858–861.

Viti, C., and Mellini, M., 1998, Mesh textures and bastites in the Elba retrograde serpentinites: European Journal of Mineralogy, v. 10, p. 1341–1359.

Walcott, R. I., 1969, Geology of the Red Hill complex, Nelson, New Zealand: Transactions of the Royal Society of New Zealand, Earth Sciences, v. 7, p. 57–88.

White, R. S., Detrick, R. S., Sinha, M. C., and Cormier, M. H., 1984, Anomalous seismic structure of oceanic fracture zones: Geophysical Journal of the Royal Astronomical Society, v. 79, p. 779–798.

Wilson, J. T., 1954, The development and structure of the crust, *in* Kuiper, G. P., ed., The Earth as a planet: Chicago, IL, University of Chicago Press, p. 138–214.

Wunder, B., and Schreyer, W., 1997, Antigorite: high-pressure stability in the system MgO-SiO_2-H_2O (MSH): Lithos, v. 41, p. 213–227.

Wyllie, P. J., 1971, Role of water in magma generation and initiation of diapiric uprise in the mantle: Journal of Geophysical Research, v. 76, p. 1328–1338.